

Asymmetric neurotransmitter release enables rapid odour lateralization in *Drosophila*

Quentin Gaudry¹, Elizabeth J. Hong¹, Jamey Kain², Benjamin L. de Bivort^{2,3} & Rachel I. Wilson¹

In *Drosophila*, most individual olfactory receptor neurons (ORNs) project bilaterally to both sides of the brain^{1,2}. Having bilateral rather than unilateral projections may represent a useful redundancy. However, bilateral ORN projections to the brain should also compromise the ability to lateralize odours. Nevertheless, walking or flying *Drosophila* reportedly turn towards the antenna that is more strongly stimulated by odour^{3–5}. Here we show that each ORN spike releases approximately 40% more neurotransmitter from the axon branch ipsilateral to the soma than from the contralateral branch. As a result, when an odour activates the antennae asymmetrically, ipsilateral central neurons begin to spike a few milliseconds before contralateral neurons, and at a 30 to 50% higher rate than contralateral neurons. We show that a walking fly can detect a 5% asymmetry in total ORN input to its left and right antennal lobes, and can turn towards the odour in less time than it requires the fly to complete a stride. These results demonstrate that neurotransmitter release properties can be tuned independently at output synapses formed by a single axon onto two target cells with identical functions and morphologies. Our data also show that small differences in spike timing and spike rate can produce reliable differences in olfactory behaviour.

To navigate towards an odour, an insect can compare the signals from their two antennae and turn in the direction of the stronger signal. Confounding this strategy (by crossing and fixing the antennae, causing them to be spatially reversed) impairs olfactory navigation in bees, ants and locusts^{6–8}. *Drosophila* resemble other insects in using this strategy^{3–5}, but they are unlike other insects in that they have mainly bilateral ORN projections. In the *Drosophila* brain, both ipsilateral and contralateral ORN axons synapse onto antennal lobe projection neurons (PNs)⁹, and ipsilateral and contralateral synapses have approximately the same strength¹⁰. A minority of *Drosophila* olfactory glomeruli receive unilateral ORN projections^{11,11}, raising the question of whether it is the unilateral glomeruli that enable lateralization.

To investigate lateralization behaviour, we built a spherical treadmill to measure olfactory behaviour in walking *Drosophila* (Fig. 1a and Supplementary Fig. 1). To prevent the head from moving, it was glued to the body, and the two antennae were independently stimulated with odour. When we delivered fermented peach volatiles to one antenna and clean air to the other, flies on the treadmill made a fictive turn towards the odour (Fig. 1b, c). When odour or clean air was delivered symmetrically to the two antennae, flies continued to walk straight.

Fruit volatiles typically activate multiple ORN types¹². Therefore, we next used a monomolecular odour (pentanoic acid) to target a glomerulus that receives bilateral ORN input more specifically. This odour has just one known high-affinity receptor in the antenna^{11,12}. This receptor corresponds to glomerulus DM6, which receives bilateral ORN innervation^{2,9}. Pentanoic acid elicited turning behaviour as robust as that elicited by peach volatiles (Fig. 1d). Turning was significantly reduced by a mutation (*Orco*²), which silences bilateral ORNs, including the DM6 ORNs (Fig. 1d). The ORN types that project unilaterally do not express the *Orco* gene^{11,13},

and so this result implies that asymmetric input to strictly bilateral glomeruli can produce turning.

To target a single bilateral ORN type more selectively, we used an optogenetic approach (Fig. 1e). We expressed channelrhodopsin-2 (ChR2) in the ORNs that express the olfactory receptor Or42b and project to glomerulus DM1. These ORNs fired a burst of 3 or 4 spikes during a 50-ms light pulse directed at the antenna with a fine fibre-optic filament (Fig. 1f). In the same fly, light had no effect on adjacent ORNs that did not express ChR2 (Fig. 1f). Illuminating one antenna produced a turn towards the stimulus (Fig. 1g and Supplementary Fig. 2). Conversely, light offset produced a compensatory turn in the other direction (Fig. 1g, i and Supplementary Note 1). The turns evoked by ChR2 in DM1 ORNs were as large as the turns evoked by ChR2 in most ORN types (under the control of the *Orco-Gal4* line; Fig. 1h). Thus, bilateral ORNs can support lateralization behaviour, and turning can be elicited by just a few spikes per neuron in one ORN type.

The temporal control permitted by the optogenetic approach enabled us to precisely determine the latency of the behavioural response. Notably, turning began within approximately 70 ms of the ORN response onset (Fig. 1j). This is faster than the fly's stride period¹⁴ (about 100 ms, Supplementary Fig. 1). Thus, there must be a rapid mechanism in the brain for extracting lateralized information from sensory neurons.

We next asked how asymmetric odour stimuli are encoded at the level of PN spikes. We removed one antenna in order to lateralize the odour stimulus, and we made simultaneous cell-attached recordings from PNs ipsilateral and contralateral to the intact antenna (Fig. 2a, b). We recorded from pairs of PNs in the same glomerulus on different sides of the brain ('sister PNs'), using green fluorescent protein (GFP) to target our electrodes to PNs in glomerulus DM6 or DM1. We used odours that preferentially activate either DM6 ORNs or DM1 ORNs (pentanoic acid or dilute ethyl acetate¹²). In these experiments, we found a small but consistent asymmetry in PN odour responses. This was apparent in the latency to the first odour-evoked spike: the first ipsilateral spike occurred 2.47 ± 0.70 ms earlier than the first contralateral spike in DM6 PNs, and 1.01 ± 0.41 ms earlier in DM1 PNs ($n = 16$ and 6 ; Fig. 2c). The latency difference between ipsilateral and contralateral spikes was statistically significant for DM6 PN pairs, but this difference was not significant for DM1 PN pairs ($P < 0.005$ and $P = 0.06$, respectively; Wilcoxon signed-rank tests). In addition, we found an asymmetry in odour-evoked firing rates: ipsilateral firing rates were on average about 50% higher than contralateral firing rates for DM6 PNs, with a larger asymmetry for DM1 PNs (Fig. 2d–g). The asymmetry was observed even during the spontaneous firing of these cells, and it was proportionately similar for all odour concentrations (Fig. 2d, g). The asymmetry in spikes must be due to an asymmetry in synaptic currents. Indeed, asymmetric stimulation of the antennae produced systematically larger inward currents in ipsilateral versus contralateral PNs (Supplementary Fig. 3).

Synaptic currents in PNs reflect the combined effects of ORNs and local neurons, most of which release GABA (γ -aminobutyric acid)^{15–17}.

¹Department of Neurobiology, Harvard Medical School, 220 Longwood Avenue, Boston, Massachusetts 02115, USA. ²Rowland Institute, Harvard University, 100 Edwin Land Boulevard, Cambridge, Massachusetts 02142, USA. ³Department of Organismic and Evolutionary Biology and Center for Brain Science, Harvard University, 52 Oxford Street, Cambridge, Massachusetts 02138, USA.

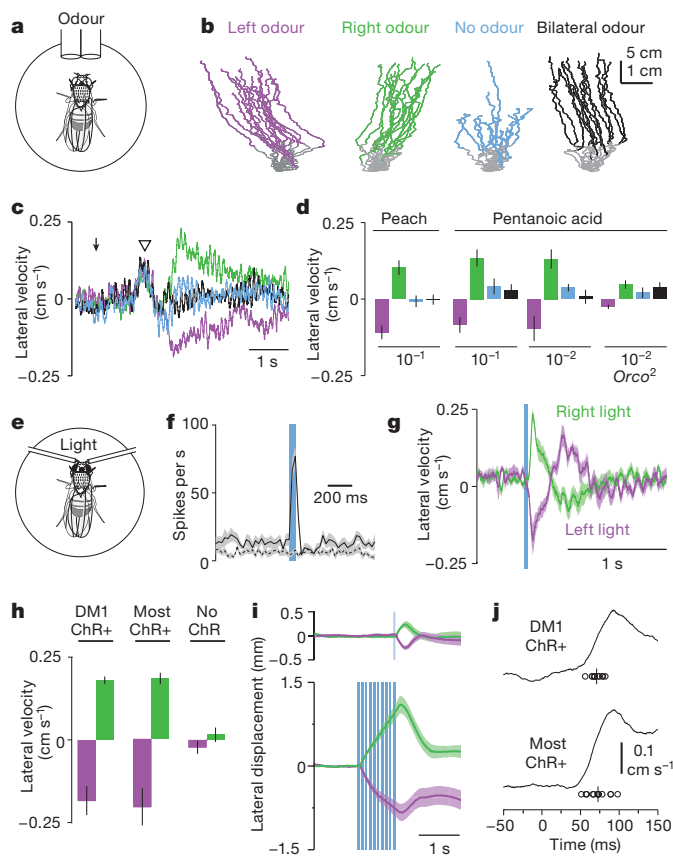


Figure 1 | *Drosophila* can lateralize odours based on bilateral receptor-neuron input to a single pair of glomeruli. **a**, Schematic diagram of a fly on a spherical treadmill, with odour tubes directed at each antenna.

b, Representative running trajectories from a single fly. Each trace is a different trial lasting 20 s. The grey portion of each trace indicates the pre-odour baseline period. Flies turn towards lateralized odour (fermented peach extract), but otherwise tend to run straight. **c**, Time course of mean lateral velocity in olfactory stimulation experiments ($n = 9$ flies). Positive values denote rightward turns and negative values denote leftward turns. Arrow indicates the onset of air flow through the tubing. The open arrowhead shows where clean air from the tip of the olfactometer first reaches the flies; this elicits a rightward turn that reflects either a systematic asymmetry in the tethering of the flies or an inherent handedness in the flies. Once this clean air is evacuated, odorized air elicits asymmetrical turning in the fly. Oscillations in lateral velocity are caused by the fly's stride rhythm (Supplementary Fig. 1). Colours as in **b**. **d**, Mean lateral velocity (\pm s.e.m.) is significantly different for right versus left odour (green versus magenta bars). This was true for peach odour (10^{-1} dilution, $P < 0.005$, $n = 9$ flies, Wilcoxon signed-rank test). It was also true for pentanoic acid (10^{-1} and 10^{-2} dilutions, $n = 8$ and 12 , $P < 0.01$ and $P < 0.005$, Wilcoxon signed-rank tests). In *Orco*² mutant flies, responses to right and left odour were still significantly different ($n = 12$ flies, $P < 0.005$, Wilcoxon signed-rank test) but were much smaller. The average difference between left and right (computed within each fly) is significantly smaller in *Orco*² flies compared to control flies ($P < 0.05$, Mann-Whitney *U*-test). The residual response in the mutants is probably due to the ORNs that do not rely on *Orco* (refs 11, 13).

e, Schematic diagram of a fly on a spherical treadmill, with a fibre-optic light guide directed at each antenna. **f**, Time course of mean light-evoked firing rate in DM1 ORNs (ChR+, solid line) versus other ORN types (ChR-, dashed line). Shaded bands here and elsewhere represent \pm s.e.m. **g**, Time course of mean lateral velocity during optogenetic stimulation in flies in which DM1 ORNs are ChR2+ **h**, Mean lateral velocity is significantly different for left and right antennal illumination in flies in which DM1 ORNs are ChR2+, or in flies in which most ORNs are ChR2+ ($n = 10$ and 12 , $P < 0.005$ and $P < 5 \times 10^{-4}$, Wilcoxon signed-rank tests), but not in flies in which no ORNs express ChR2 ($P = 0.13$, $n = 10$). To express ChR2 in most ORNs, we used the *Orco-Gal4* line. Flies that lack ChR2 expression have the *UAS-ChR2* transgene but no Gal4 transgene. **i**, Time course of mean lateral displacement in response to a single light pulse (top) or a train of pulses (bottom). After the train, the magnitude of the compensatory turn is larger ($P < 0.005$, *t*-test), but the flies are also significantly less accurate in returning to their original running trajectory ($P < 0.005$, *t*-test). **j**, Time course of absolute mean lateral velocity on an expanded scale around the time of light onset (0 ms). Open circles show the turning latency for each fly. The mean latency across flies is shown as a vertical bar.

We asked whether the asymmetry in PN activity requires GABAergic inhibition, by bath-applying GABA_A and GABA_B receptor antagonists. These antagonists elevated PN firing rates, but the difference between ipsilateral and contralateral PN firing rates was not significantly altered (Fig. 3a, b).

Our results suggest that the asymmetry originates at the level of ORN input to PNs. To compare ORN–PN synapses in ipsilateral versus contralateral PNs, we made simultaneous whole-cell recordings of spontaneous excitatory postsynaptic currents (sEPSCs) in pairs of sister PNs. These sEPSCs are known to arise from ORN–PN synapses^{9,10}. Each ORN–PN synapse consists of many release sites with high release probability, and spike-evoked synaptic events are therefore large and reliable¹⁰. In recordings from sister PNs in glomerulus DM6, almost all sEPSCs occurred in a paired fashion (Fig. 3c). Almost 100% of the sEPSCs in one cell had a corresponding paired event in the other cell, and this percentage was not significantly different in ipsilateral versus contralateral PNs ($98.3 \pm 0.6\%$ versus $96.4 \pm 1.3\%$, $n = 15$ pairs, $P = 0.11$; Wilcoxon signed-rank test). This result indicates that the number of unitary ORN–PN synaptic connections is essentially identical on the ipsilateral and contralateral sides, and it also indicates that action-potential conduction failures do not occur to any notable degree in the contralateral axon branches of ORNs, although we cannot completely exclude the idea that this occurs at a low rate.

These dual whole-cell recordings enable us to measure the mean difference in ipsilateral versus contralateral sEPSC arrival times (0.80 ± 0.51 ms). The difference in arrival times represents the delay imposed by axonal conduction between sister glomeruli. This delay is less than the delay between the first contralateral odour-evoked spike and the first ipsilateral odour-evoked spike in glomerulus DM6 (2.47 ms, see above). This makes sense, because the difference in first spike times is the result of two delays: the delay imposed by axonal conduction and the delay that results from less net synaptic excitation in the contralateral PN (Supplementary Fig. 3), which means that

the contralateral PN requires more integration time to reach spike threshold.

Comparing the amplitude of paired sEPSCs on an event-by-event basis, we found considerable variation in the relative amplitude of ipsilateral versus contralateral EPSCs (Fig. 3d). This is expected, given that synaptic vesicle release is a stochastic process occurring independently at ipsilateral and contralateral synapses. When many sEPSCs were considered together, there was a consistent asymmetry in the amplitude of sEPSCs (Fig. 3d). Averaged across all experiments, ipsilateral sEPSCs were 39% larger in amplitude than their contralateral counterparts (Fig. 3e). Thus, although ORN spikes reliably invade both ipsilateral and contralateral axon branches, each ORN spike typically has a stronger effect on ipsilateral PNs.

In principle, the asymmetry in sEPSC amplitudes could have either a pre- or postsynaptic locus. To determine whether we can observe this asymmetry at the level of presynaptic release sites, we expressed synaptobrevin–GFP (a marker of presynaptic release sites) in DM6 ORNs. We removed one antenna and allowed 3 days for the cut ORN axons to degenerate, leaving only the axons from the intact antenna. We found that total synaptobrevin fluorescence was on average $41 \pm 16\%$ higher on the ipsilateral side, and the ipsilateral:contralateral ratio of synaptobrevin fluorescence was significantly greater than 1 ($P < 0.05$, $n = 5$, *t*-test, Fig. 4a). This suggests an asymmetry in the number or size of neurotransmitter release sites. This is consistent with a previous study reporting that a plasma membrane marker

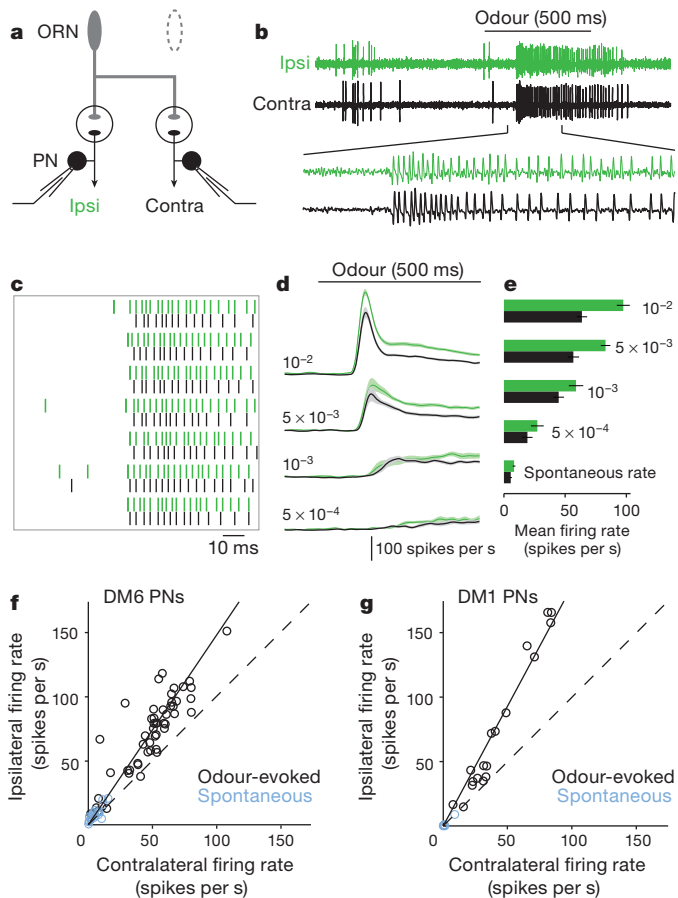


Figure 2 | Lateralized odours produce an asymmetry in spike latency and spike rate in antennal lobe PNs. **a**, Schematic of the set up for simultaneous cell-attached recording. An ORN axon innervates a glomerulus on each side of the midline, where it synapses onto postsynaptic PNs. In these experiments, one antenna was removed to lateralize the odour. **b**, Sample cell-attached recordings from a pair of PNs (postsynaptic to glomerulus DM6). The odour stimulus is a 500-ms pulse of pentanoic acid (10^{-2} dilution). Enlarged segment below is 250 ms. **c**, Raster plot showing the spiking responses of ipsilateral and contralateral DM6 PNs (odour is pentanoic acid at 10^{-2} dilution). Each pair of rows represents a single trial from the same pair of neurons. The raster starts 180 ms after the nominal odour-pulse onset. Note the shorter ipsilateral latency (see text). **d**, Time course of mean firing rates of DM6 PNs to a descending series of pentanoic acid concentrations. **e**, Mean firing rates of DM6 PNs (\pm s.e.m.) in response to pentanoic acid concentrations. Spontaneous rates are also shown. Mean rate is computed over a 500-ms period starting 100 ms after the olfactometer is activated ($n = 16, 15, 10, 10$ and 21 pairs, in descending order of concentration). **f**, Trial-averaged ipsilateral versus contralateral firing rates for DM6 PNs. Several odour concentrations were used in each experiment, and each point represents a different experiment-concentration combination. Note that the ipsilateral–contralateral difference is present in spontaneous activity (blue symbols). Significance was assessed by fitting a line through the origin to the data for each individual experiment; these slopes were significantly different from unity (mean slope = 1.47 ± 0.09 , $P < 10^{-4}$, Mann–Whitney U -test, $n = 21$ experiments). The dashed line is unity; the solid line is the mean of all linear fits in the individual experiments. **g**, Same as **f**, but for DM1 PNs (mean slope = 1.86 ± 0.04 , $P < 0.05$, Mann–Whitney U -test, $n = 6$ experiments). Odour stimuli were ethyl acetate at 10^{-12} , 10^{-10} and 10^{-6} dilutions. In DM1 PNs, spontaneous firing rates are close to zero.

was more abundant on the ipsilateral side¹⁸. In that study, 1 antenna was severed and imaging was performed 3 days later, as here. Functional remodelling can occur in that time period^{18,19}, so both findings should be interpreted cautiously.

Next, to visualize presynaptic calcium, we expressed the genetically encoded calcium indicator GCaMP3.0 in ORNs (using the *pebbled-Gal4*

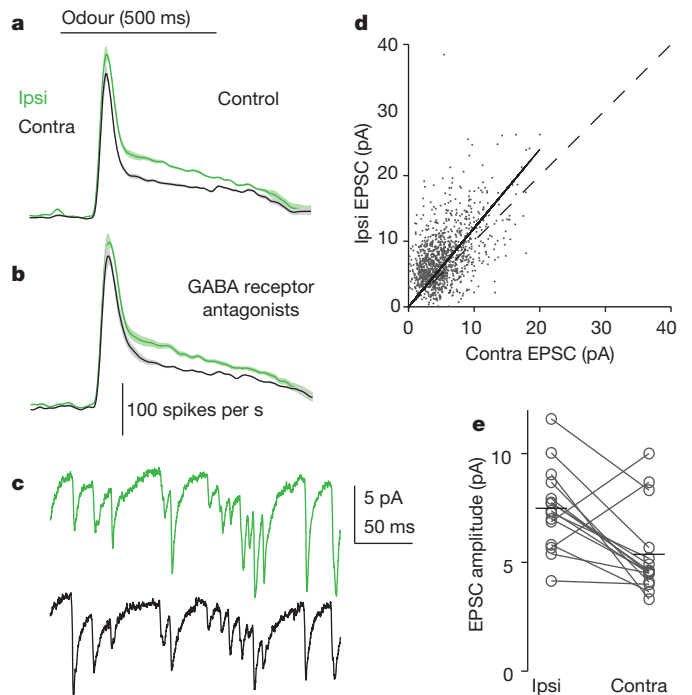


Figure 3 | The asymmetry arises at the level of ORN–PN synapses. **a**, Mean DM6 PN responses to pentanoic acid (10^{-2} dilution) in normal saline. **b**, Same as **a**, but with the addition of the GABA_A receptor antagonist picrotoxin (5 μ M) and the GABA_B receptor antagonist CGP54626 (50 μ M). Ipsilateral firing rates are significantly higher than contralateral rates ($P < 0.01$), and the antagonists have no significant effect on the ipsilateral–contralateral difference ($P = 0.86$, $n = 10$, two-way analysis of variance (ANOVA) on data from **a** and **b**). The ipsilateral–contralateral difference in peak firing rates becomes somewhat smaller, but because this occurs only at the peak, it is probably due to the near-saturation of PN firing rates. **c**, Whole-cell recordings of sEPSCs from a pair of DM6 PNs. The PN ipsilateral to the intact antenna is in green. **d**, Ipsilateral versus contralateral EPSC amplitudes in a typical pair of DM6 PNs. Each point represents a pair of sEPSCs ($n = 1,213$). Dashed line is unity; solid line is a linear fit constrained to intersect the origin. **e**, Group data showing mean sEPSC amplitudes in all pairs of DM6 PNs. Each symbol is a different experiment and horizontal lines represent means across experiments. sEPSC amplitudes are significantly larger in ipsilateral PNs ($n = 15$ pairs, $P < 0.05$, Wilcoxon signed-rank test).

line) and used two-photon microscopy to visualize calcium signals in ORN axon terminals. To lateralize the odour, we removed one antenna immediately before the experiment (Fig. 4b). We used pentanoic acid to evoke a fluorescence increase preferentially in glomerulus DM6 (Fig. 4c). We found that the size of the calcium response was significantly greater on the side of the brain ipsilateral to the intact antenna (Fig. 4c, d). This asymmetry did not require feedback from central circuits, because it persisted after washing in mecaminylamine (to block nicotinic acetylcholine receptors, which mediate ORN–PN synaptic transmission¹⁰) along with picrotoxin and CGP54626 hydrochloride (GABA_A and GABA_B receptor antagonists, respectively) (Fig. 4e). In separate experiments, we saw similarly asymmetric calcium signals in glomerulus DL5, using an odour stimulus that is relatively selective for DL5 ORNs²⁰ (trans-2-hexenal, 10^{-5} dilution, data not shown). We also saw a similar asymmetry in presynaptic currents, using simultaneous bilateral field potential recordings (Supplementary Fig. 4). Together, these results demonstrate that the asymmetry in EPSC amplitudes has a presynaptic origin.

Interestingly, we found a roughly equal asymmetry ($\sim 40\%$) in the amplitude of sEPSCs, the level of synaptobrevin fluorescence, and the odour-evoked GCaMP3 fluorescence change. The simplest explanation for these results is that the ipsilateral arbor is 40% larger than the contralateral arbor. If everything else is equal, then this mechanism

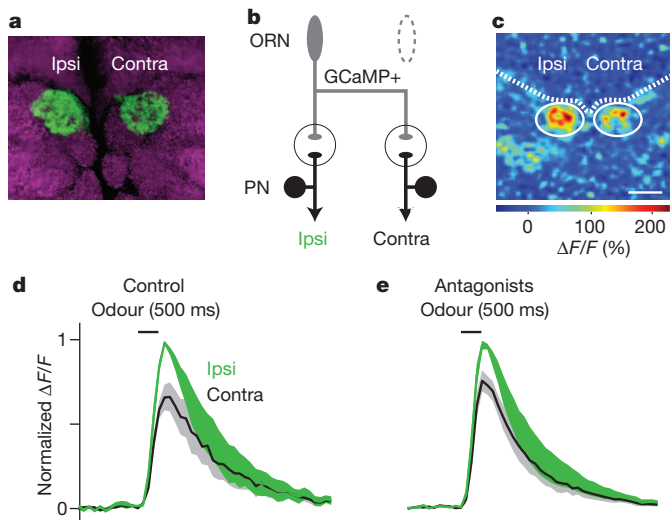


Figure 4 | The asymmetry in ORN–PN synapses has a presynaptic origin. **a**, Synaptobrevin–GFP (green) was expressed in DM6 ORNs to label neurotransmitter release sites, and 1 antenna was removed 3 days before to allow the cut axons to degenerate. The brain is viewed from the anterior face. Magenta shows neuropil contours (nc82 immunofluorescence). Scale bar, 10 μ m. **b**, Schematic of calcium-recording configuration. ORNs express GCaMP, and one antenna was removed to lateralize the odour. **c**, Changes in fluorescence in ORN axon terminals in response to pentanoic acid (10^{-2} dilution). Solid circles outline the DM6 glomeruli, and the dashed line shows the anterior boundary of the antennal lobe neuropil. The brain is viewed from the dorsal side. Scale bar, 10 μ m. **d**, Mean time course of odour-evoked calcium signals in ORN axons innervating glomerulus DM6. Black bar indicates the timing of the odour stimulus (pentanoic acid at 10^{-2} dilution, 500 ms). **e**, Same as **d**, except after adding picrotoxin, CGP54626, and the nicotinic receptor antagonist mecamylamine (200 μ M). Ipsilateral responses are significantly larger than contralateral responses ($P < 0.05$) and the antagonists have no significant effect on the ipsilateral–contralateral difference ($P = 0.75$, $n = 6$, two-way ANOVA on data from panels **d** and **e**).

should produce a proportional change in all these measurements (Supplementary Note 2).

Our results are consistent with the finding that in flies with one antenna removed, 2-deoxyglucose uptake is higher on the side ipsilateral to the intact antenna²¹. A previous study using calcium imaging has reported that asymmetric ORN stimulation can produce stronger signals in ipsilateral PNs than in contralateral PNs²², which is also broadly consistent with our results. However, in contrast to our results, this asymmetry was restricted to just a few glomeruli. This finding is puzzling, given that a variety of stimuli can produce turning behaviour (Fig. 1 and refs 3–5). The same study also concluded that GABAergic inhibition mediates the ipsilateral–contralateral asymmetry in PNs²². These discrepancies may reflect limitations of the imaging techniques used in that study, as well as differences between stimuli or glomeruli.

Another previous study failed to find any significant ipsilateral–contralateral differences in the strength of ORN–PN synapses¹⁰. However, the measurements in the study involved sequential recordings from sister PNs, rather than simultaneous recordings, and the measurements were of EPSCs arising from a single ORN per PN. Here we have better statistical power because we have made simultaneous recordings from sister PNs, and because we sampled sEPSCs arising from many ORNs. Our finding that ipsilateral and contralateral synapses differ only modestly explains why this difference has been difficult to resolve previously.

It is well-known that a single axon can form neurotransmitter release sites with different properties on different postsynaptic cell types (for example, principal neurons versus interneurons²³). Here we have shown that ORN axons discriminate between two classes of target cells (left and right) that are morphologically and functionally

identical, and that share the same lineage and birth dates²⁴. This is reminiscent of the circuitry of the leech midbody ganglion, in which individual mechanoreceptor axons make stronger synapses onto ipsilateral versus contralateral sister cells that are otherwise functionally identical²⁵. It is possible that these target cells may be distinguished because right and left sister neurons express different molecular tags²⁶, thereby allowing a given axon to recognize them as ipsilateral versus contralateral in relation to itself. Alternatively, an axon might form more release sites at proximal locations than at distal locations; this cell-intrinsic mechanism would suffice because contralateral sites are always more distal than ipsilateral sites.

Our results reveal that even small signals in the *Drosophila* nervous system can be behaviourally relevant. The stimuli we used in our optogenetic experiments produced only a slight fractional difference in input to the right and left sides of the brain. This difference amounted to 5% over the 50-ms stimulus period (Supplementary Note 3). The finding that this incremental difference is relevant for behaviour should provide an additional motive for the continued development of sensitive methods for monitoring neural activity in the fly brain.

METHODS SUMMARY

The odour-delivery device used for the olfactory behavioural experiments was specially designed to deliver no lateralized mechanical cues, and we carried out control experiments to confirm that no turning was observed when no odour was present (Supplementary Fig. 5). The spherical treadmill apparatus was constructed by floating a small plastic sphere on a jet of compressed air. We measured the forward velocity (pitch) and lateral velocity (roll) of the sphere in the apparatus by placing the sensor from an optical mouse underneath the sphere. Photostimulation of *Drosophila* ORNs was achieved by butt-coupling a blue light-emitting diode (LED) to a fibre-optic filament (50 μ m diameter) and positioning the tip of the fibre approximately 150 μ m away from the fly's antenna. In all behavioural experiments using light to stimulate ORNs, the eyes and ocelli of the fly were shielded from light by painting them with ink. *In vivo* extracellular recordings from ORNs and patch-clamp recordings from PNs were carried out as described previously^{9,27}. In all electrophysiology or calcium-imaging experiments (except ORN recordings), one antenna was removed just before the experiment by a person who was not the experimenter, and the experimenter remained blind to which side of the brain was ipsilateral to the intact antenna. All analysis was also carried out blind to which side was ipsilateral. Calcium-imaging experiments were performed on a custom-built two-photon microscope. All aggregated data represent mean \pm s.e.m. computed across experiments. See Supplementary Methods for details on the spherical treadmill, odour delivery, optogenetic stimuli and analysis of sEPSCs.

Full Methods and any associated references are available in the online version of the paper.

Received 6 May; accepted 7 November 2012.

Published online 23 December 2012.

1. Stocker, R. F., Lienhard, M. C., Borst, A. & Fischbach, K. F. Neuronal architecture of the antennal lobe in *Drosophila melanogaster*. *Cell Tissue Res.* **262**, 9–34 (1990).
2. Couto, A., Alenius, M. & Dickson, B. J. Molecular, anatomical, and functional organization of the *Drosophila* olfactory system. *Curr. Biol.* **15**, 1535–1547 (2005).
3. Borst, A. & Heisenberg, M. Osmotropotaxis in *Drosophila melanogaster*. *J. Comp. Physiol. A* **147**, 479–484 (1982).
4. Duistermars, B. J., Chow, D. M. & Frye, M. A. Flies require bilateral sensory input to track odor gradients in flight. *Curr. Biol.* **19**, 1301–1307 (2009).
5. Flugge, C. Geruchliche raumorientierung von *Drosophila melanogaster*. *Z. Vgl. Physiol.* **20**, 463–500 (1934).
6. Kennedy, J. S. & Moorhouse, J. E. Laboratory observations on locust responses to wind-borne grass odour. *Entomol. Exp. Appl.* **12**, 487–503 (1969).
7. Martin, H. Osmotropotaxis in the honey-bee. *Nature* **208**, 59–63 (1965).
8. Hangartner, W. Spezifität und inaktivierung des spurpheromons von *Lasius fuliginosus* (Latr.) und orientierung der arbeiterinnen im dufffeld. *Z. Vgl. Physiol.* **57**, 103–136 (1967).
9. Kazama, H. & Wilson, R. I. Origins of correlated activity in an olfactory circuit. *Nature Neurosci.* **12**, 1136–1144 (2009).
10. Kazama, H. & Wilson, R. I. Homeostatic matching and nonlinear amplification at genetically-identified central synapses. *Neuron* **58**, 401–413 (2008).
11. Silbering, A. F. *et al.* Complementary function and integrated wiring of the evolutionarily distinct *Drosophila* olfactory subsystems. *J. Neurosci.* **31**, 13357–13375 (2011).

12. Hallem, E. A. & Carlson, J. R. Coding of odors by a receptor repertoire. *Cell* **125**, 143–160 (2006).
13. Benton, R., Vannice, K. S., Gomez-Diaz, C. & Vosshall, L. B. Variant ionotropic glutamate receptors as chemosensory receptors in *Drosophila*. *Cell* **136**, 149–162 (2009).
14. Strauss, R. & Heisenberg, M. Coordination of legs during straight walking and turning in *Drosophila melanogaster*. *J. Comp. Physiol. A* **167**, 403–412 (1990).
15. Chou, Y. H. *et al.* Diversity and wiring variability of olfactory local interneurons in the *Drosophila* antennal lobe. *Nature Neurosci.* **13**, 439–449 (2010).
16. Okada, R., Awasaki, T. & Ito, K. Gamma-aminobutyric acid (GABA)-mediated neural connections in the *Drosophila* antennal lobe. *J. Comp. Neurol.* **514**, 74–91 (2009).
17. Das, A. *et al.* *Drosophila* olfactory local interneurons and projection neurons derive from a common neuroblast lineage specified by the empty spiracles gene. *Neural Dev.* **3**, 33 (2008).
18. Berdnik, D., Chihara, T., Couto, A. & Luo, L. Wiring stability of the adult *Drosophila* olfactory circuit after lesion. *J. Neurosci.* **26**, 3367–3376 (2006).
19. Kazama, H., Yaksi, E. & Wilson, R. I. Cell death triggers olfactory circuit plasticity via glial signaling in *Drosophila*. *J. Neurosci.* **31**, 7619–7630 (2011).
20. Olsen, S. R., Bhandawat, V. & Wilson, R. I. Divisive normalization in olfactory population codes. *Neuron* **66**, 287–299 (2010).
21. Rodrigues, V. Spatial coding of olfactory information in the antennal lobe of *Drosophila melanogaster*. *Brain Res.* **453**, 299–307 (1988).
22. Agarwal, G. & Isacoff, E. Specializations of a pheromonal glomerulus in the *Drosophila* olfactory system. *J. Neurophysiol.* **105**, 1711–1721 (2011).
23. Pelkey, K. A. & McBain, C. J. Differential regulation at functionally divergent release sites along a common axon. *Curr. Opin. Neurobiol.* **17**, 366–373 (2007).
24. Jefferis, G. S., Marin, E. C., Stocker, R. F. & Luo, L. Target neuron prespecification in the olfactory map of *Drosophila*. *Nature* **414**, 204–208 (2001).
25. Lockery, S. R. & Kristan, W. B. Jr. Distributed processing of sensory information in the leech. II. Identification of interneurons contributing to the local bending reflex. *J. Neurosci.* **10**, 1816–1829 (1990).
26. Chintapalli, V. R. *et al.* Functional correlates of positional and gender-specific renal asymmetry in *Drosophila*. *PLoS ONE* **7**, e32577 (2012).
27. Bhandawat, V., Olsen, S. R., Schlieff, M. L., Gouwens, N. W. & Wilson, R. I. Sensory processing in the *Drosophila* antennal lobe increases the reliability and separability of ensemble odor representations. *Nature Neurosci.* **10**, 1474–1482 (2007).

Supplementary Information is available in the online version of the paper.

Acknowledgements We are grateful to M. Dickinson, V. Jayaraman, L. Luo, D. Tracey and L. Vosshall for gifts of fly stocks. A. Baker helped construct and improve the spherical treadmill apparatus. Members of the Wilson laboratory provided feedback on the manuscript. This work was supported by a research project grant from the National Institutes of Health (R01DC008174). R.I.W. is an HHMI Early Career Scientist. B.L.d.B. and J.K. were supported by the Rowland Junior Fellows Program.

Author Contributions Q.G. and R.I.W. designed the experiments. Q.G. carried out all of the experiments, except for the calcium imaging, which was performed by Q.G. and E.J.H., and the synaptobrevin imaging, which was performed by R.I.W. Q.G. analysed the data. J.K. and B.L.d.B. helped to design and build the spherical treadmill apparatus. Q.G. and R.I.W. wrote the manuscript.

Author Information Reprints and permissions information is available at www.nature.com/reprints. The authors declare no competing financial interests. Readers are welcome to comment on the online version of the paper. Correspondence and requests for materials should be addressed to R.I.W. (rachel_wilson@hms.harvard.edu).

METHODS

For all electrophysiology and calcium-imaging experiments, each stimulus was presented in 4 to 6 trials, and the responses were averaged together to produce the response for that experiment. Before statistical tests, all the data in a given panel were collectively tested for normality using a Shapiro–Wilk test. If the data were not normally distributed, then a non-parametric test was used for all the comparisons in that panel.

Fly stocks. Flies (1 to 2 days post eclosion) were raised on conventional cornmeal medium at 25 °C with a 12 h light–dark cycle. For behavioural experiments, we used a fly stock recently derived from wild-caught *Drosophila melanogaster* (provided by M. Dickinson), because these flies showed more robust running than inbred stocks. For optogenetic experiments, we used flies with one copy of the *Gal4* transgene and two copies of the *UAS-ChR2-YFP* transgene (one on chromosome 2 and one on chromosome 3). All flies harbouring the *UAS-ChR2-YFP* transgene, including control flies lacking the *Gal4* transgene, were raised on food containing all-trans retinal. All-trans retinal was prepared as a stock solution in ethanol (35 mM), and 10 µl of this stock was mixed into approximately 5 ml of rehydrated potato flakes and added to the top of a vial of conventional food. DM6 PN recordings were carried out using the genotype *NP3062-Gal4,UAS-CD8-GFP*. DM1 PN recordings were carried out using the genotype *NP5221-Gal4,UAS-CD8-GFP*. Synaptobrevin-imaging experiments were carried out in the genotype *Or67d-Gal4/UAS-n-syb-eGFP*. Calcium-imaging experiments were carried out in the genotype *pebbled-Gal4/UAS-GCaMP3.0*. Fly stocks were previously published as follows: wild-caught flies²⁸, *Or42b-Gal4* (ref. 29, Bloomington no. 9971), *Orco-Gal4* (*Or83b-Gal4*, ref. 30, Bloomington no. 26818), *UAS-ChR2-YFP* (ref. 31), *NP3062-Gal4* (ref. 10, DGRC no. 113083), *NP5221-Gal4* (ref. 32, DGRC no. 104906), *UAS-CD8-GFP* (ref. 33, Bloomington no. 5136 and no. 7465), *Or67d-Gal4* (ref. 2, Bloomington no. 23904), *UAS-n-syb-eGFP* (ref. 34, Bloomington no. 6921), *pebbled-Gal4* (ref. 35), *UAS-GCaMP3.0* (ref. 36, Bloomington no. 32116), *Orco*² (ref. 30, Bloomington no. 23130). For details on the spherical treadmill, odour delivery and optogenetic stimulation, see Supplementary Methods.

ORN recordings. Extracellular recordings from ORNs were conducted as described previously². In brief, the fly was mounted on the end of a cut pipette tip and secured using paraffin wax. The third antennal segment was restrained using hooks fabricated from glass capillaries positioned with micromanipulators. Specific ORN types were identified based on the size and location of the sensillum, together with the action potential wave forms and odour responses of the ORNs. ChR2-expressing ORNs were stimulated using the same fibre-optic apparatus used in the behavioural experiments. To verify that the light from the fibre-optic cables was sufficiently focused, we also recorded from ChR2-expressing ORNs in the antenna contralateral to the illumination, and we confirmed that these neurons showed no responses to light (data not shown). The bins in Fig. 1f are 25-ms wide and are plotted versus the time that corresponds to the end of each bin.

PN recordings. Flies were dissected as described previously²⁷, except that the odour source was lateralized by removing one antenna just before recording. The identity of the intact antenna was pseudo-randomized between preparations. We targeted our electrodes to particular PNs by expressing GFP in these PNs (see the section on fly stocks above). The identity of each recorded PN was confirmed using a panel of diagnostic odours, and was corroborated in pilot studies using immunohistochemistry to identify the glomerulus innervated by the PN dendrites. Data were low-pass filtered at 1 kHz for cell-attached recordings and at 5 kHz for whole-cell recordings using an Axopatch 200B amplifier (Molecular Devices) and digitized at 10 kHz. The external saline was prepared as described previously²⁷ and was continuously bubbled with a blend of 95% O₂ and 5% CO₂. Whole-cell experiments were carried out in voltage-clamp mode with a holding potential of –60 mV. The internal solution contained (in mM) caesium aspartate, 140; HEPES, 10; MgATP, 4; Na₃GTP, 0.5; EGTA, 1; CsCl, 1; biocytin hydrazide, 13

(pH 7.3, osmolarity adjusted to ~265 mOsm). Cell-attached recordings were carried out in voltage-clamp mode and the command potential was adjusted so that the amplifier did not pass any current. For cell-attached recordings, we used patch pipettes filled with either external saline or the internal pipette solution used for the whole-cell recordings. As both DM6 PNs and DM1 PNs have low spontaneous firing rates, the identification of the first spike in the odour response was generally unambiguous. To ensure that the first-spike latency was measured in an unbiased way, we used an automated algorithm to identify the first spike after odour onset; this was defined as the spike preceding the first inter-spike interval that is shorter than 90% of the inter-spike intervals in the pre-odour period. For details on the analysis of sEPSCs, and on synaptobrevin-imaging, see Supplementary Methods.

Calcium imaging. We expressed the genetically encoded calcium indicator GCaMP3.0 in olfactory receptor neurons using the Gal4/UAS system. We used flies homozygous for both *UAS-GCaMP3.0* and *pebbled-Gal4*, which drives expression in most or all ORNs (along with other antennal neurons that do not project to the antennal lobe). These flies were older than those used in the rest of the study (25 to 35 days post eclosion) because we found that this increased GCaMP3.0 fluorescence. Just before each experiment, one antenna was removed to lateralize the odour. The olfactometer was identical to the one used for electrophysiology experiments. The inter-trial interval was 45 s. Data were collected on a custom-built two-photon microscope at a frame rate of 7.8 Hz. Images were collected at each of several *z* planes that collectively spanned the depth of the DM6 glomeruli, and all these images were averaged together and filtered with a two-dimensional Gaussian (s.d. = 5 pixels). The odour-evoked increase in fluorescence was determined by drawing a region of interest around the activated glomeruli in the sequence of raw fluorescence images. We then calculated the change in fluorescence divided by the baseline fluorescence ($\Delta F/F$) within this region for each frame. The peak calcium signal was measured from odour onset through the next 5 frames (640 ms total). All imaging experiments and analyses were carried out blind with regard to which antenna was removed. Resting fluorescence (*F*) was not significantly different in the ipsilateral and contralateral glomeruli. Although there are probably more release sites on the ipsilateral side (Fig. 4a), any asymmetry in resting fluorescence resulting from spontaneous activity is evidently too small to resolve. In these experiments, we did not detect a fluorescence increase outside of the expected glomeruli, except for a relatively weak and intermittent signal in DM1; however, DM1 also responded when replaced the odour vial with an empty vial, indicating that it was responding to a contaminant in our delivery system rather than the odour.

28. Bhandawat, V., Maimon, G., Dickinson, M. H. & Wilson, R. I. Olfactory modulation of flight in *Drosophila* is sensitive, selective and rapid. *J. Exp. Biol.* **213**, 3625–3635 (2010).
29. Fishilevich, E. & Vosshall, L. B. Genetic and functional subdivision of the *Drosophila* antennal lobe. *Curr. Biol.* **15**, 1548–1553 (2005).
30. Larsson, M. C. *et al.* *Or83b* encodes a broadly expressed odorant receptor essential for *Drosophila* olfaction. *Neuron* **43**, 703–714 (2004).
31. Hwang, R. Y. *et al.* Nociceptive neurons protect *Drosophila* larvae from parasitoid wasps. *Curr. Biol.* **17**, 2105–2116 (2007).
32. Tanaka, N. K., Awasaki, T., Shimada, T. & Ito, K. Integration of chemosensory pathways in the *Drosophila* second-order olfactory centers. *Curr. Biol.* **14**, 449–457 (2004).
33. Lee, T. & Luo, L. Mosaic analysis with a repressible cell marker for studies of gene function in neuronal morphogenesis. *Neuron* **22**, 451–461 (1999).
34. Zhang, Y. Q., Rodesch, C. K. & Broadie, K. Living synaptic vesicle marker: synaptotagmin-GFP. *Genesis* **34**, 142–145 (2002).
35. Sweeney, L. B. *et al.* Temporal target restriction of olfactory receptor neurons by Semaphorin-1a/PlexinA-mediated axon-axon interactions. *Neuron* **53**, 185–200 (2007).
36. Tian, L. *et al.* Imaging neural activity in worms, flies and mice with improved GCaMP calcium indicators. *Nature Methods* **6**, 875–881 (2009).